

Mission Architecture for the Green Propulsion Dual Mode Mission

Kevin Tong, Samuel Wood, Mohit Singh, Conner Awald, Rithvik Nagarajan, Briana Paul, Dev Gujarathi,
E. Glenn Lightsey

Georgia Institute of Technology Space Systems Design Laboratory
620 Cherry St NW, Atlanta, GA 30332; 908-294-1001
ktong37@gatech.edu

Nehemiah J. Williams, Christopher G. Burnside, Beau C. Simpson
NASA Marshall Space Flight Center
Martin Rd SW, Huntsville, AL 35808

ABSTRACT

Current spacecraft propulsion technologies are broadly divided into chemical and electric propulsion modes, each of which has unique advantages. It is common for both systems to have a place in interplanetary spacecraft, but the size, weight, and power required to carry two separate propulsion systems is extremely limiting for small spacecraft such as CubeSats. The upcoming NASA STMD-funded Green Propulsion Dual Mode (GPDM) mission will demonstrate on-orbit a novel dual-mode propulsion system known as the GPDM Propulsion System that uses the AF-M315E/ASCENT green monopropellant to feed both a chemical 100 mN monopropellant thruster and four electrospray thrusters. GPDM will fly a 6U CubeSat in low Earth orbit and perform orbit-raising and lowering maneuvers to characterize the performance of this dual-mode propulsion technology, enabling a new generation of future interplanetary small satellite explorers.

The Georgia Institute of Technology Space Systems Design Laboratory (SSDL) is conducting the design, assembly, integration, testing, and mission operations of the GPDM host spacecraft, as well as the integration of the GPDM Propulsion System payload, designed by NASA's Marshall Spaceflight Center (MSFC). The NASA Marshall Space Flight Center is overseeing the overall GPDM project as well as specific technology development activities of the GPDM Propulsion System, while electrospray thrusters are supplied by the MIT Space Propulsion Lab, with additional components supplied by MMA Design, Blue Canyon Technologies, Quasonix, Xiphos, and Rubicon Space Systems. The GPDM spacecraft will carry the GPDM Propulsion System into orbit and use a high-power S-band radio to enable real-time operations in low Earth orbit (LEO) via the NASA Tracking and Data Relay Satellite System (TDRSS). The mission is working towards a tentative launch readiness date of August 2025, in support of launch and operations commencing in January 2026. This paper describes GPDM's overall mission concept of operations, spacecraft overview, and subsystem breakdown.

1 Introduction

Spacecraft propulsion is generally separated into two broad categories: 1) chemical propulsion and 2) electric propulsion. Chemical propulsion technologies include monopropellant, bipropellant, hybrid, solid, and warm/cold-gas systems. These systems provide a relatively large amount of thrust and are relatively inefficient due to the low exhaust velocity of the accelerated reaction masses. Therefore, these systems are limited in total delivered ΔV by their total propellant load and low specific impulses. Fig. 1 shows schematic diagrams of several chemical propulsion systems. On the other hand, electric propulsion technologies such as gridded ion, Hall-

effect, pulsed plasma, and electrospray thrusters. These systems use electric power to increase propellant exhaust velocity instead of a chemical reaction and can achieve much higher specific impulse (Isp) than chemical propulsion systems, which is advantageous for station-keeping, orbital maintenance, and interplanetary transfer. However, electric propulsion systems deliver very low thrust, and therefore cannot be used when large impulses are required by a mission architecture such as an orbit insertion in a short time frame. Fig. 2 shows schematic diagrams of several types of electric propulsion technology^{1,2,3}

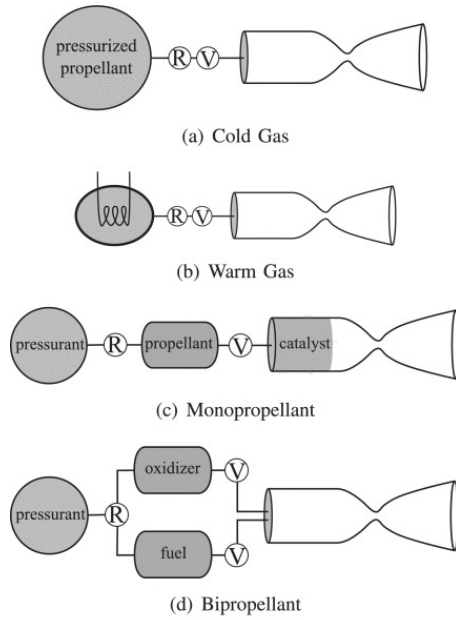


Figure 1: Schematic diagrams of a selection of chemical propulsion systems.³

CubeSats are small satellites that can be deployed from a range of standardized containers which allow for their launch as secondary payloads that pose limited risk to the launch vehicles' primary payload. These spacecraft have rapidly proliferated, with the number of CubeSats launched being well over 2200 as of October 2023.⁴ Importantly, due to their typical launch mode being as auxiliary payloads, CubeSat missions, especially those targeting non-standard orbits, typically do not have the same degree of control over initial trajectory as traditional sole-payload missions.⁵

The increasing capability and demonstrated utility of miniaturized spacecraft over recent years has led to a desire to use CubeSats for lunar, interplanetary, and other deep space missions. The first interplanetary CubeSats were the twin Mars Cube One (MarCO) spacecraft, which were subsequently followed by several others, mostly launched into cislunar space. These interplanetary CubeSats have all been deployed from primary payloads on a trajectory to a similar destination, although in some cases limited propulsive maneuvers for trajectory correction have been performed, such as the successful maneuvers performed by the MarCO and EQUULEUS missions using cold-gas and water resistojet systems respectively.^{6,7,8}

In larger modern interplanetary spacecraft, high-performance electric propulsion often provides the primary source of ΔV to enable transfer to a target body, while separate chemical systems are used for

orbital insertion. For instance, the Dawn spacecraft used xenon gridded-ion thrusters for its interplanetary transfers, while an array of hydrazine thrusters were carried for orbital insertion and attitude control.^{9,10} However, in a small spacecraft context, the size, weight, and power (SWaP) required by two separate propulsion systems is difficult to support, which dramatically limits the capabilities of CubeSat missions. This issue is particularly compounded by the tendency of CubeSat insertions to be dictated by the primary payload, which tends to drive missions into convoluted trajectory design where the ability to both have high ΔV transfer and high impulse maneuvering capability would greatly improve mission science and technical results.¹¹

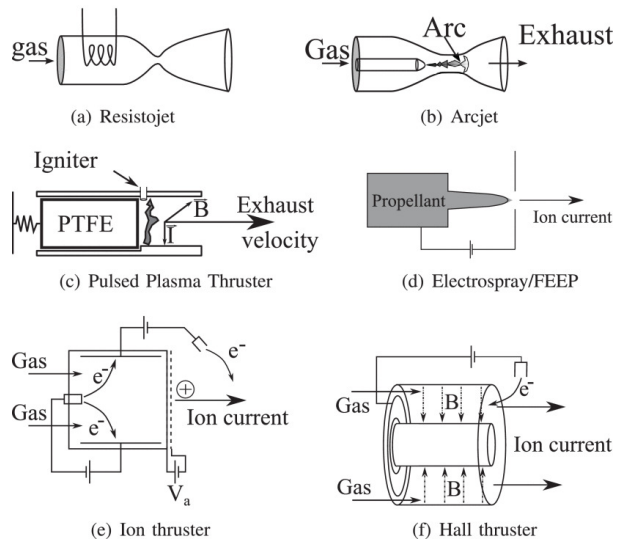


Figure 2: Schematic diagrams of a selection of electric propulsion systems.³

In recent years, a push to develop so-called "green monopropellants" which are less toxic than the hydrazine traditionally used in monopropellant thrusters has led to propellants which are hydroxylammonium nitrate (HAN) based ionic liquid at room temperature. These ionic liquid compounds, in particular the Advanced SpaceCraft Energetic Non-Toxic (ASCENT) propellant, also known as AF-M315E, are capable of being used as the propellant for low-thrust electro spray thrusters as well as the impulsive monopropellant systems which they were originally developed for.¹¹ The Green Propellant Dual Mode (GPDMD) mission is a new program funded by the NASA Space Technology Mission Directorate (STMD) which aims to demonstrate a dual-mode propulsion payload on-orbit using a 6U CubeSat.

2 GPDM Mission Overview and Concept of Operations

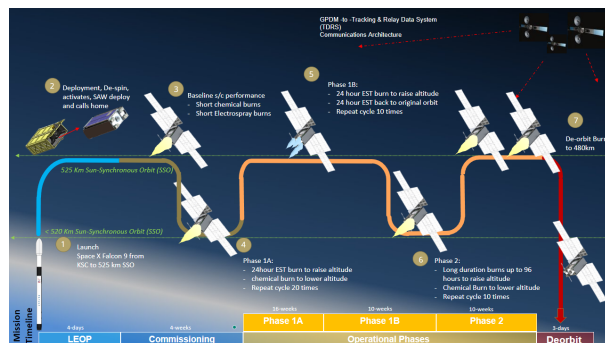


Figure 3: GPDM Concept of Operations.

The objective of the GPDM mission is to demonstrate dual-mode monopropellant and electroprayer propulsion in orbit. In pursuit of this mission, the primary spacecraft payload is the GPDM Propulsion System using the ASCENT propellant. GPDM is a collaboration between the NASA Marshall Space Flight Center (MSFC), the Massachusetts Institute of Technology's Space Propulsion Laboratory (SPL), and the Georgia Institute of Technology's Space Systems Design Laboratory (SSDL). The mission project office is located at MSFC, the SPL provides the electroprayer thrusters, and the SSDL is responsible for propulsion system integration, spacecraft bus design and integration, and mission operations. The NASA Small Spacecraft Technology program manages the GPDM project.

The concept of operations (CONOPS) for GPDM is shown in Fig. 3. After launch, the spacecraft deploys from a dispenser on the second stage of the launch vehicle into a low Earth orbit. The current baseline is a 520-525 km sun-synchronous orbit (SSO), although the mission is intended to be able to advantage of a wide variety of rideshare launch opportunities. The spacecraft will autonomously undergo initial deployment, boot-up, de-tumbling, solar panel deployment, and then establish a comms link. Operators perform subsystem checkouts, which brings the launch and early operations (LEOP) phase to a close.

Following LEOP, spacecraft commissioning will begin and last for 4 weeks, being broken up into a 2 weeks commissioning of the chemical propulsion system, a one-week test period for short-duration electroprayer thruster operations, followed by one week of long-duration electroprayer operations.

Nominal operations will then begin. The currently proposed communications architecture involves the use of daily contact with the spacecraft

via the NASA Near Space Network's (NSN) Tracking and Data Relay Satellite System (TDRSS). During real-time operations, limited data is relayed to the operators in real-time, while higher-fidelity payload data is stored for later downlink. Further details of nominal operations will be detailed in Section 4. Finally, at the end of mission life, the spacecraft's remaining fuel will be expended to bring the mission to a low enough altitude to enable atmospheric reentry. The mission is currently scheduled to launch no earlier than (NET) Q4 2025.

3 Spacecraft Overview

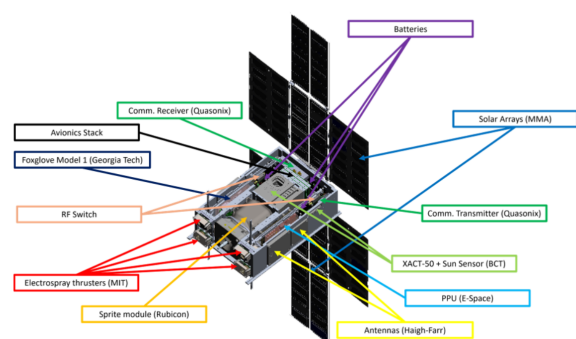


Figure 1: GPDM Spacecraft overview

Figure 4: GPDM spacecraft bus showing major subsystems.

The GPDM spacecraft is a 6U CubeSat designed to be launched via a tab-type CubeSat dispenser. The major spacecraft subsystems are the attitude determination and control system (ADCS), the communications system (COMM), the command and data handling system (C&DH), and the electrical power system (EPS). The spacecraft's technology demonstration payload is the GPDM Propulsion System, which includes a single Sprite integrated chemical propulsion module, four electroprayer thrusters, and a compact pressure reduction system (CPRS) which interfaces between Sprite and the electroprayers. Fig. 4 shows the spacecraft with major subsystem components labeled - details of each system are discussed in the following sections.

3.1 GPDM Propulsion System

The GPDM Propulsion System is a dual-mode propulsion system that draws upon elements of two previous CubeSat-scale propulsion systems and combines them with a common propellant tank. The chemical portion of GPDM Propulsion System uses the same 100 mN ASCENT thruster used in the Lunar Flashlight Propulsion System (LFPS) developed

by MSFC which was integrated at the SSDL before launch.¹²

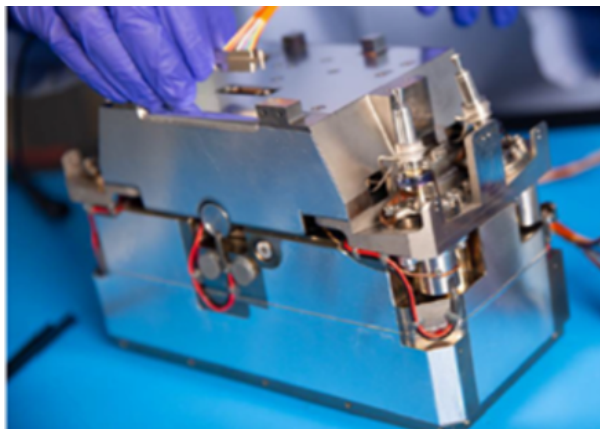


Figure 5: The flight-qualified LFPS in the SSDL clean room¹

In the case of GPDM, there is only a single 100 mN thruster mounted center-line on the spacecraft's long thrust axis as part of a Sprite propulsion system supplied by Rubicon Space Systems which integrates the 100 mN thruster, ASCENT propellant tank, propellant management devices, Foxglove Model 2 chemical propulsion controller, and control valves. Foxglove Model 2 was previously developed by the SSDL.

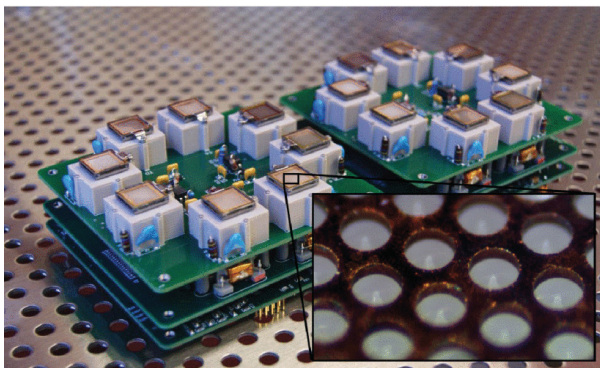


Figure 6: EDUs for the MIT electro spray propulsion system showcasing the emitter arrays.³

The Sprite structure is made from additively manufactured titanium and operates in a blow-down feed mode. An auxiliary propellant feed port allows propellant delivery to the electro spray thrusters. The 100 mN thruster has a steady-state Isp of 215 s and 1200 Ns of total impulse under purely chemical propulsion. Typical pressures in the chemical propulsion feed system run between 275 psi. The chemical system uses heaters to keep the propellant at temperature and to pre-heat the catalyst bed in

the thruster to greater than 400 °C^{13,14}

The electric propulsion system used in GPDM Propulsion System is the ion Electro spray Propulsion System (iEPS) under development at the MIT SPL. Using ASCENT propellant, the iEPS has previously been shown to produce 5-20 μ N of thrust with an Isp of 1800-2800 s. The iEPS thrusters use propellant reservoirs to store their propellant and operate in near-vacuum conditions, with a 10 psi upper limit. A Power Processing Unit (PPU) developed by Espace, Inc. delivers the +/- 2.0 kV of electric potential at +/- 350 μ A required for ion acceleration.¹¹

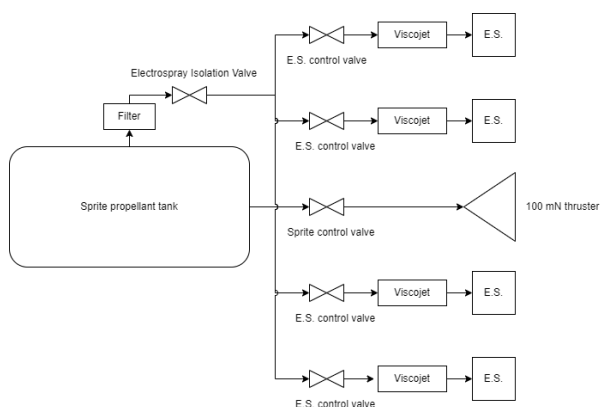


Figure 7: Functional block diagram of the GPDM Propulsion System.

The CPRS is the connecting link between the Sprite tank and the electro spray thrusters. Fig. 7 shows a functional block diagram of the GPDM Propulsion System, wherein the CPRS makes up the propellant delivery and pressure reduction lines between the Sprite tank and the electro spray thrusters.

The system features a single isolation valve mounted in a manifold block, followed by four individual thruster valves mounted in paired manifolds that control the flow of propellant to each electro spray thruster. These valves are flight-proven, having previously flown on LFPS. The manifolds on the two sides of the Sprite module are connected via steel tubing welded onto the blocks, while the final stretch from the manifold blocks to the electro spray fittings uses Teflon tubing to ensure electrical isolation of the iEPS thrusters. Filters are placed upstream of each valve to reduce foreign object debris (FOD) risk, and Lee Company ViscoJet compact multi-orifice restrictors are used to reduce the system pressure from the 250 psi of Sprite down to the 10 psi operating pressure of the iEPS thrusters.

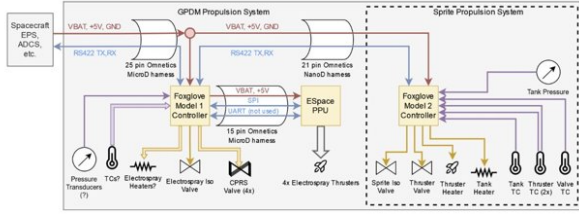


Figure 8: Block diagram of the GPDM Propulsion System control scheme.

Finally, the overall GPDM Propulsion System controller is called Foxglove Model 1, developed by the SSDL. Foxglove Model 1 controls Sprite as well as all four electro spray thrusters and the five CPRS control valves. The controller is radiation-hard and has interfaces with the Sprite Foxglove Model 2 controller as well as the valves and PPU. The rest of the spacecraft interfaces with the GPDM Propulsion System via a single RS-422 line located on Foxglove Model 1. 5V and 12V power lines for the GPDM Propulsion System are also routed through Foxglove Model 1.

Software for the controller is written using the JPL-developed F' flight software framework. As of summer 2024, flatsat testing of the GPDM Propulsion System control system using flight-like avionics and simulators of peripherals such as valves, thermocouples, heaters, e-spray thrusters, and the chemical thruster is well underway. Flight software Revision 1 for the GPDM Propulsion System is also complete.

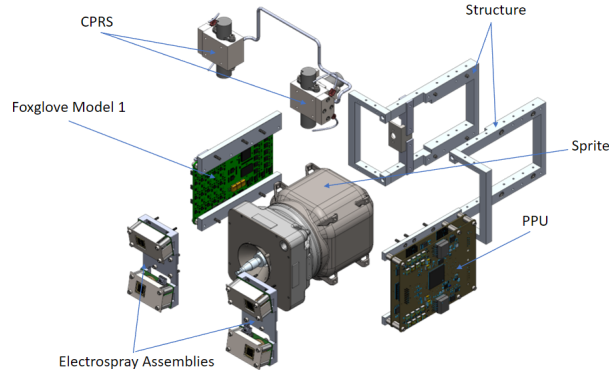


Figure 9: CAD exploded view of the GPDM Propulsion System.

Fig. 9 shows a CAD view of the GPDM Propulsion System integrated payload, with the PPU facing the viewer and Foxglove Model 1 mounted across from it. The Sprite chemical propulsion system is the large additively manufactured module in the center of the image. The large manifolds on the side of Sprite are the isolation and electro spray control valves, with the Viscojets integrated into the manifolds. Teflon tubing (not shown) connects the exit of

the manifolds to the fittings on the end of the iEPS thrusters.

3.2 Attitude Determination and Control System

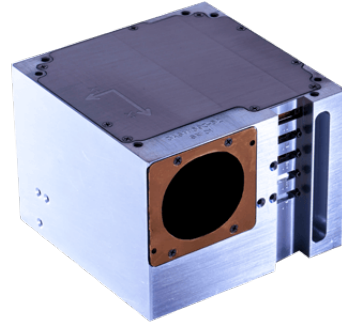


Figure 10: BCT XACT-50 integrated ADCS system.¹⁵

GPDM requires a robust ADCS system to point the spacecraft's thrust axis for maneuvers. The selected ADCS system for GPDM is the Blue Canyon Technologies (BCT) XACT-50, which integrates a star tracker, reaction wheels, torque rods, GPS receiver, and coarse sun sensors. The XACT-50 will determine spacecraft position and velocity from GPS data (L1/L2), provide pointing for both chemical and electro spray maneuvers, and use its star tracker and coarse sun sensors to determine spacecraft attitude.

The XACT-50's onboard torque rods will provide the primary means for reaction wheel unloading, with the GPDM Propulsion System's electro spray thrusters providing an additional means of desaturation. Unlike on the Lunar Flashlight mission, GPDM will not use the XACT-50 as a pass-through to command the propulsion system to allow for more direct control in support of its technology demonstration mission^{12, 15}.

3.3 Communications

The GPDM communication architecture was primarily driven by the direction to use NASA-affiliated assets through the Space Communication and Navigation (SCaN) and the technical project PI's desire for real-time operation of the spacecraft in a "joystick" mode, wherein spacecraft operators will be able to have more direct control over the spacecraft in case of unexpected events during the technology demonstration. Several communication architectures were investigated, including commercial direct-to-Earth (DTE), NASA asset-provided DTE,

and space relay (SR). Ground-pass and link budget analysis was performed to evaluate the options, with the major criteria being the total number of available contacts, total contact time, and total data downlink over the 9-month nominal mission. Fig. 12 shows a block diagram of the integrated communications architecture.

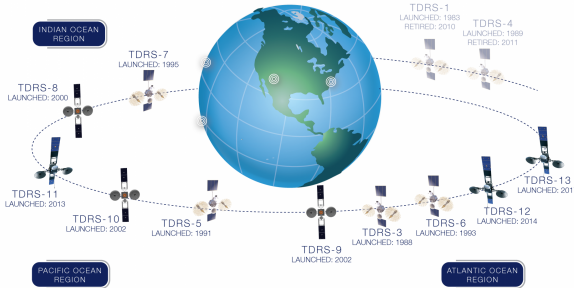


Figure 11: The current fleet of TDRS satellites operated by NASA, comprising the space segment of the NSN.¹⁶

A combination of the request for real-time control and program costing estimates led to the selection of a SCaN-operated SR architecture using the Tracking and Data Relay Satellite (TDRS) single-access (SA) service as the primary communications system for GPDM. Signals from the mission operations center (MOC) at the SSDL will be routed via SCaN as a bent pipe through the TDRSS in geostationary orbit down to GPDM and vice-versa. To conform to government mission resilience standards, FIPS-140 encryption is implemented in software to protect commands.

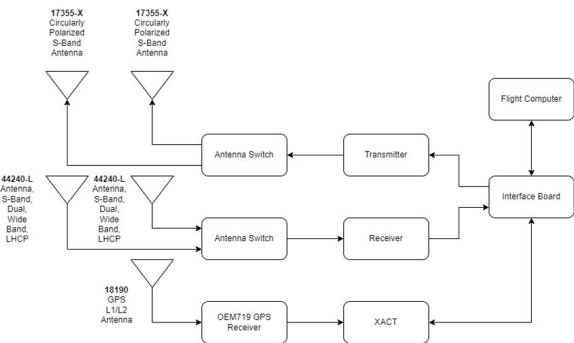


Figure 12: GPDM communications system schematic.

The primary communication system of the GPDM project is a high-power S-band transmitter and receiver developed by Quasonix. The TIMTER transmitter allows for frequency tuning in 0.5 MHz steps between 2200.5 MHz to 2300.5 MHz, supporting a wide variety of modulation schemes including

BPSK, QPSK, OQPSK, and UQPSK. Using a built-in solid-state power amplifier, the transmitter supports a maximum of 10 W RF or +40.0 dBm transmit power with a power draw of 32 W at 28 V.¹⁷



Figure 13: Quasonix TIMTER compact transmitter.¹⁷

Meanwhile, the RDMS single-channel compact receiver can receive between 2025 MHz to 2110 MHz with the same variety of modulations with a noise figure of 3.5 dB. The RDMS draws 21 W of sustained power at 28 V.¹⁸ The RDMS incorporates a built-in low-noise amplifier (LNA). Both systems have significant flight heritage on launch vehicles. Fig. 13 and Fig. 14 show manufacturer-provided images of TIMTER and RDMS S-band units.

The integrated communications system incorporates both Quasonix Rx and Tx units, which send and receive signals from the spacecraft flight computer via the IO interface board, as well as an RF front end and two sets of S-band antennas in the corresponding frequencies.



Figure 14: Quasonix RDMS compact receiver.¹⁸

Link budget analysis for the downlink from GPDM via TDRS to the ground was performed using the general free-space link budget equation in

the log domain, where E_b is energy per bit, N_0 is the noise figure, EIRP is the Equivalent Isotropic Radiated Power, L_s is the free path space loss, $\frac{G_t}{T}$ is the gain to noise temperature ratio, DR is the data rate, and L_{margin} is the link margin.¹⁹

$$\frac{E_b}{N_0}(dB) = EIRP(dBW) - L_s(dB) + \frac{G_t}{T}(\frac{dB}{K}) + 228.6dB - 10 * \log(DR_{bps}) - L_{margin} \quad (1)$$

$\frac{E_b}{N_0}$ is set to be 10 dB, which corresponds to a bit rate error of roughly $1e-5$ for QPSK modulation, which is usable on a spread-spectrum TDRS system^{20, 19}. The equation for EIRP is as follows:

$$EIRP = P_{emitted}(dBW) + G_{antenna}(dB) - L_{pointing} - L_{system} \quad (2)$$

Using the system parameters of transmitter power $P_{emitted} = 7.8dBW$, assumed antenna gain $G_{antenna} = 5dB$, assumed pointing loss $L_{pointing} = 1.0dB$, and assumed additional system line losses of $L_{system} = 0.5$, spacecraft EIRP is determined to be $14.8dBW$. Free-space path loss $L_s(dB)$ is determined using the following equation:

$$L_s(dB) = 92.45 + 20\log(d) + 20 * \log(f) \quad (3)$$

$L_s = -191dB$ using a baseline median transmit frequency f of 2.25 GHz and a distance d of 40000 km, which accounts for some passage past the Earth's disk. The TDRS SA service has a $\frac{G}{T}$ figure of $9/5 \frac{dB}{K}$.²⁰ With this analysis, the primary S-band system supports telemetry downlink data rates of up to 25 kbps via TDRS SA with a link margin of 15.4 dB. A similar analysis shows command uplink rates of 25 kbps with a total link margin of 9.4 dB.

Owing to the high real-time data rates which can be achieved using the TDRS data relay system, high-fidelity 1 Hz telemetry is able to be streamed to mission operators on all subsystems. During critical activities such as chemical burns and propellant refills, 4Hz data for fluid system sensors may be streamed in real-time. Overall, the communications architecture of the GPDM mission enables a real-time spacecraft-to-ground integrated link with sufficient margin using the TDRS data relay service with adequately high data rates to enable GPDM's intended real-time operations mode.

3.4 Command and Data Handling

The C&DH system for GPDM receives commands from the ground, forwards real-time and

stored telemetry back, and interfaces with all other subsystems. The primary flight computer is the Xiphos Q7S, a radiation-hard flight computer with considerable flight heritage that incorporates both a dual-core ARM processor and a pair of FPGAs for IO and watchdog functionality. The GPDM flight software (FSW) deployment will be onboard the Q7S.

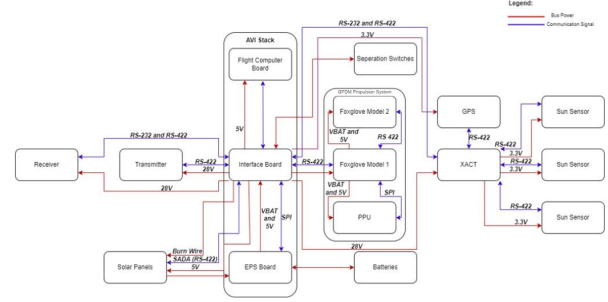


Figure 15: GPDM avionics integrated interface diagram.

The Q7S communicates with the other spacecraft subsystems via the IO interface board, which also routes power using electrical pass-throughs. Fig. 15 shows an interface diagram of the integrated GPDM avionics system, with power and communications lines with the relevant mechanical connections highlighted. The interface board, along with the Q7S and the EPS, forms the GPDM bus avionics (AVI) stack. The primary method of communication is via RS-422 serial communication, although the Iridium transmitter uses the older RS-232 line. Serial communication lines that are beyond the standard 2 RS-422 lines aboard the ARM processor are implemented in the Q7S IO FPGA and are physically connected to the IO interface board.

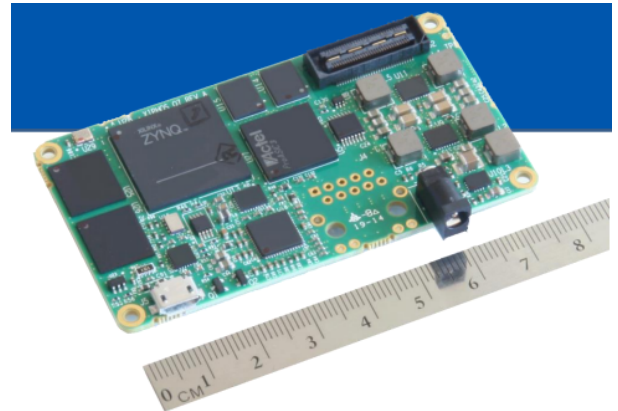


Figure 16: Xiphos Q7S rad-hardened flight computer.²¹

The Q7S's processing capability allows for the

use of a Linux-based deployment of the JPL F' framework as the core architecture, which implements many common spacecraft functionalities by default. The GPDM FSW is organized around a general state manager, and various subsystem manager components receive commands from and send telemetry to the general state manager. Each subsystem manager is then linked via subsystem IO to the subsystem controllers to perform commanded actions. Fig. 17 shows the top-level GPDM F' deployment block diagram, with built-in F' components shown in yellow and custom GPDM components in green.

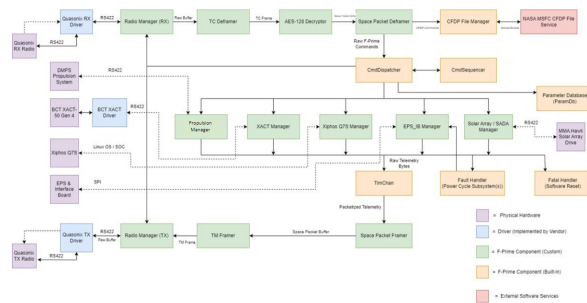


Figure 17: GPDM flight software functional diagram, with GPDM-specific component highlighted in green.

A notable set of FSW components is the sequence of components that manage spacecraft-to-ground communications. This set of components includes the radio manager, telemetry framer/deframer, and decrypter components. All inter-subsystem and space-to-ground communication follows the Space Packet Protocol established by the Consultative Committee for Space Data Systems (CCSDS).²²

A telemetry packet received by the receiver and initially processed by the radio driver will pass via RS-422 serial channel through the interface board to the flight software, where it will be initially handled by the radio manager. The radio manager outputs a bitstream to the TC Deframer component, which extracts CCSDS telecommand (TC) packets. The TC packet fields are then decrypted, and the FSW determines if the telemetry packet received is a command or file packet, which is then forwarded to either the F-Prime Command Dispatcher or the onboard File Service manager respectively. Downlink from the spacecraft is handled effectively in the reverse manner, although the packets use the CCSDS telemetry (TM) protocol.

Ground-side command and telemetry data send, receive, and encryption are handled by the Tele-science Resource Kit (TReK) ground data system

(GDS), which was originally developed for use by ISS payloads.²³

3.5 Electrical Power System

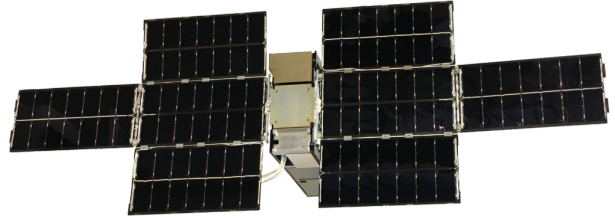


Figure 18: MMA 112 W LunaH-map derived deployable solar array.²⁴

The EPS for GPDM consists of three major components: the EPS regulation board, the spacecraft batteries, and the deployable solar arrays. The EPS regulation board is a part of the overall GPDM AVI stack which provides 5V and unregulated battery power to the rest of the bus. The board charges the batteries from the solar panels, balances individual cell charges inside of the batteries to maximize battery lifetime, and provides telemetry of the EPS system state.

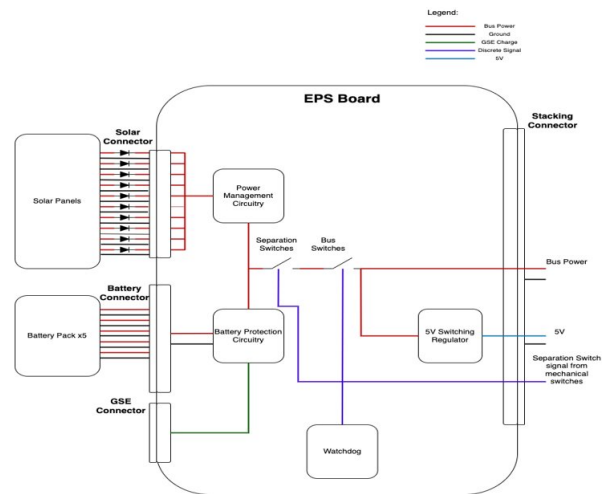


Figure 19: GPDM EPS board diagram.

The development of a new EPS board by the SSDL in support of the large power requirements of the GPDM mission and also represents a major increase in the capabilities of the SSDL to support high-performance CubeSat missions. The GPDM EPS has a primary purpose of providing the spacecraft bus with both regulated 5V and unregulated battery voltage (10.8V-12.6V). To support this mission, the EPS utilizes cell balancing to charge the batteries selectively to increase battery longevity, while also incorporating features such as individual

switches that allow for on/off control of individual subsystems and a watchdog circuit round out the features of the EPS board. Fig. 19 shows a block diagram of the EPS board. As of mid-spring 2024, the EPS board is in its second design revision, with functional testing nearly complete.

The individual battery packs of GPDM are modeled after the systems flown on Lunar Flashlight and each consists of three commercial 18650-series lithium-ion batteries connected in series via conductive nickel strips to allow for bus battery voltage between 12.6V and 10.8V. The three batteries are secured within an aluminum housing for structural and modal resilience, with temperature probes and heaters attached to the outside of the heat-conductive housing. Finally, a small PCB is mounted atop each battery pack, feeding all power lines, sensors, and heating elements for each cell.

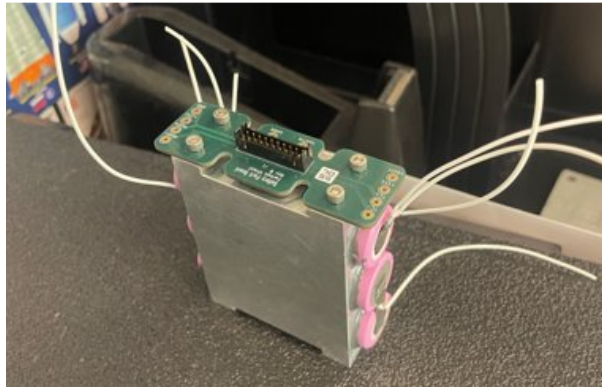


Figure 20: GPDM battery pack EDU during initial assembly. Note that

These cells are then wired in parallel via the EPS board to enable a modular arrangement of the spacecraft battery. A five-battery pack configuration with a total energy storage of 16750 mAh was chosen for the mission, allowing for maximum endurance during eclipses and off-nominal situations. This configuration is effectively fifteen 18650-series cells in a 3-series 5-parallel configuration. Fig. 20 shows a prototype version of an individual battery pack before testing.

Power budget analysis showed that the primary drivers of spacecraft power consumption are the S-band transmitter (32 W), the S-band receiver (21 W), and the GPDM Propulsion System (up to 18.31 W during short chemical maneuvers). The MMA Design eHaWK 27AS112, which previously flew on the Artemis I Lunar Polar Hydrogen Mapper (LunaH-Map) mission, was selected as the primary solar array.²⁴ This system provides 112 W of peak power, which is sufficient across a full orbit to sup-

port the 89.4 W power draw of the spacecraft in its most high-power operating mode without the need for any charging orbits to replenish depleted batteries between mission activities. This rapid cadence is necessary due to the constrained mission timeline of 9 months and limited daily access to TDRS SA service.

4 Mission Operations

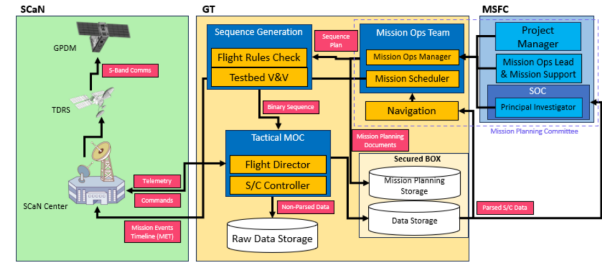


Figure 21: GPDM mission operations information flow diagram.

The development of the operational documents for GPDM is currently in early development. SSDL is drawing on previous experiences operating the Lunar Flashlight spacecraft for NASA to develop the GPDM Mission Operations Plan (MOP).²⁵ Fig. 21 shows the mission operations information flow envisioned for GPDM, wherein a core group of student controllers who make up the core GPDM operations team serves as the interface between program management and the principal investigator at MSFC and the GPDM spacecraft via the telecommunications link provided by NASA SCA-N assets.

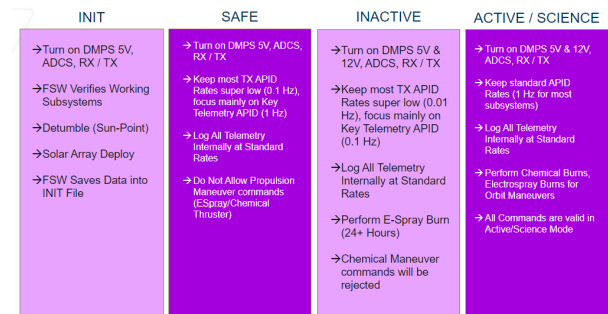


Figure 22: GPDM state diagram showing the spacecraft primary software states.

Georgia Tech SSDL will serve as the primary mission operations center (MOC) for GPDM. Operators assigned to the MOC serve simultaneously as spacecraft flight directors and controllers in "tactical" operations, a role in which they control the

spacecraft in real-time according to pre-planned activities. Meanwhile, these same operators will plan out future command sequences and procedures by participating in activity planning. All new activities are then subjected to verification and validation using the GPDM spacecraft testbed. When those future activities are acted on in the tactical MOC, the operators who took the lead in developing the plan for the spacecraft's upcoming activity will serve as the flight director while the activity is underway.

Fig. 22 shows the spacecraft's primary states. The nature of GPDM as a technology demonstration mission in which direct operator control over the propulsion module payload is desired leads to a simplified onboard state machine. After launch, the spacecraft deploys into the INIT state, in which systems turn on, subsystems are checked out, the vehicle detumbles, and the solar arrays are deployed. In the INIT state, the spacecraft receiver powers on, and under three-axis control, the vehicle awaits ground direction via TDRS. Fig. 23 shows a more detailed view of autonomous flight software actions in the INIT state.

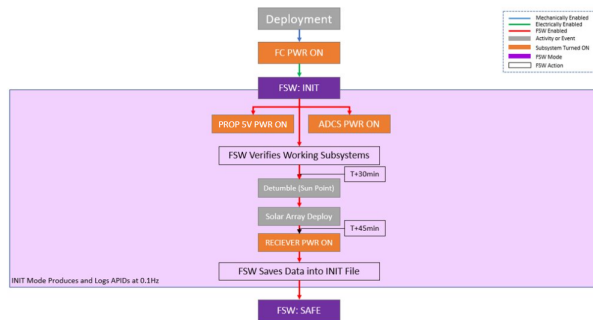


Figure 23: GPDM flight software state diagram during a launch and early operations (LEOP).

After the initiation of contact with the spacecraft operators, the spacecraft switches itself into the ACTIVE/SCIENCE state, in which all commands sent are directly performed by the spacecraft, and the ground controllers directly "joystick" the vehicle. Notably, a real-time telemetry stream of 1Hz is sent to operators via TDRS and chemical burn commands to the GPDM Propulsion System are enabled in this mode. Sequences uploaded for electric propulsive maneuvers extending beyond a single ground contact may continue into the INACTIVE state. Fig. 24 shows the activation diagram of this state.

Between contacts after deployment, the spacecraft is kept in the INACTIVE state, in which the spacecraft transmits low-rate telemetry and performs any long-duration electric propulsion maneu-

vers that may have been sent in the last contact.

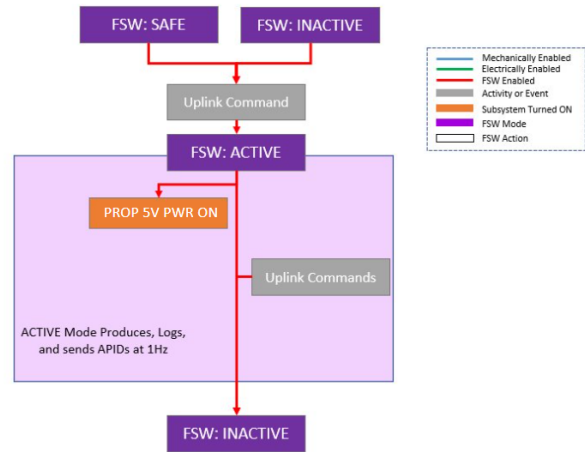


Figure 24: GPDM flight software state diagram during a delta-v maneuver sequence.

Data products such as orbit parameters, subsystem health telemetry, and high-fidelity thruster sensor data downlinked from the spacecraft will be generated by the TRK GDS and post-processing tools built on top of TRK, to be distributed to the GPDM principal investigator at MSFC.

5 Conclusion

This paper describes the initial design and systems engineering development of NASA's Green Propulsion Dual Mode mission. The GPDM Propulsion System blends the components from previous successful missions in chemical and electric propulsion to produce a novel hybrid system that puts the advantages of both systems in a CubeSat-sized package. The Georgia Tech SSDL is now preparing for the mission's critical design review before spacecraft assembly, integration, and testing begin. Subsystem EDUs are currently undergoing developmental testing and assembly of the GPDM flatsat testbed is underway. Based on current schedules, GPDM will fly the first dual-mode propulsion system and be the first CubeSat to be operated via the TDRS in late 2025, blazing the trail for a new era of interplanetary explorers.

Acknowledgments

This material is based upon work supported by the National Aeronautics and Space Administration grant 80NSSC21K0870.

References

- [1] Bruce Yost and Sasha Weston. *Small Spacecraft Technology State of the Art Report*. NASA Ames Research Center Small Spacecraft Systems Virtual Institute, 'Jan' 2023.
- [2] Dan M Goebel, Ira Katz, and Ioannis G Mikelides. *Fundamentals of electric propulsion*. John Wiley & Sons, 2023.
- [3] David Krejci and Paulo Lozano. Space propulsion technology for small spacecraft. *Proceedings of the IEEE*, 106(3):362–378, 2018.
- [4] Erik Kulu. Nanosats database. Web, Oct 2023. Accessed 9 Dec 2023.
- [5] Richard P. Welle. *Overview of CubeSat Technology*, pages 1–17. Springer International Publishing, Cham, 2020.
- [6] Josh Schoolcraft, Andrew Klesh, and Thomas Werne. *MarCO: Interplanetary Mission Development on a CubeSat Scale*, pages 221–231. Springer International Publishing, Cham, 2017.
- [7] Benjamin K. Malphrus, Anthony Freeman, Robert Staehle, Andrew T. Klesh, and Roger Walker. 4 - interplanetary cubesat missions. In Chantal Cappelletti, Simone Battistini, and Benjamin K. Malphrus, editors, *Cubesat Handbook*, pages 85–121. Academic Press, 2021.
- [8] Ryu Funase, Shintaro Nakajima, Serhat Altunc, Yosuke Kawabata, Ryota Fuse, Hokuto Sekine, and Hiroyuki Koizumi. Equuleus: Initial operation results of an artemis-1 cubesat to the earth—moon lagrange point. In '*Small Satellite Conference*', 2023. 'SSC23-WVII-03'.
- [9] Christopher Russell, Maria Barucci, Richard Binzel, Maria Capria, U. Christensen, Angioletta Coradini, Maria Cristina De Sanctis, W.C. Feldman, Ralf Jaumann, Horst Keller, Alexander Konopliv, Thomas Mccord, Lucy Mcfadden, Kevin Mckeegan, Harry McSween, Stefano Mottola, A. Nathues, Gerhard Neukum, C.M. Pieters, and Maria Zuber. Exploring the asteroid belt with ion propulsion: Dawn mission history, status and plans. *Advances in Space Research*, 40:193–201, 12 2007.
- [10] Valerie C. Thomas, Joseph M. Makowski, G. Mark Brown, John F. McCarthy, Dominick Bruno, J. Christopher Cardoso, W. Michael Chiville, Thomas F. Meyer, Kenneth E. Nelson, Betina E. Pavri, David A. Termohlen, Michael D. Violet, and Jeffrey B. Williams. *The Dawn Spacecraft*, pages 175–249. Springer New York, New York, NY, 2012.
- [11] Amelia R. Bruno and Paulo C. Lozano. Design and testing of a propellant management system for bimodal chemical-electrospray propulsion. In *2021 IEEE Aerospace Conference (50100)*, pages 1–7, 2021.
- [12] Celeste Smith, Nathan Cheek, Christopher Burnside, John Baker, Philippe Adell, Frank Picha, Matthew Kowalkowski, and E Glenn Lightsey. The journey of the lunar flashlight propulsion system from launch through end of mission. In *Proceedings of the Small Satellite Conference SSC23-VI-03*, 2023.
- [13] Mackenzie Kilcoin, Daniel Cavender, Tomas Hasanof, Michael Zaluki, Tim McKechnie, Corinne Sedano, and Hunter Williams. Development of ascent propellant thrusters and propulsion systems. *Proceedings of the Small Satellite Conference*, 2022.
- [14] Rubicon Space Systems. Sprite propulsion system. Web, n.d. Accessed 9 Dec 2023.
- [15] Blue Canyon Technologies. Components. Web, n.d. Accessed 10 Dec 2023.
- [16] Pete Vrotsos Kul Bhasin and Eli Naffah. Commercial communication services for nasa space missions: Capability assessment, opportunities and challenges. In *Ka Band Conference*, 2020.
- [17] Quasonix. Timter transmitters. Web, n.d. Accessed 10 Dec 2023.
- [18] Quasonix. Rdms compact receivers. Web, n.d. Accessed 10 Dec 2023.
- [19] David F. Everett Wertz, James Richard and Jeffery John Puschell. *Space Mission Engineering: The New SMAD*. Microcosm Press, 2011.
- [20] Exploration and Space Communications Project Division. Near space network. Web, 2022. Accessed 13 Dec 2023.
- [21] Xiphos Technologies. Q7s specifications. Web, n.d. Accessed 11 Dec 2023.
- [22] Consultative Committee for Space Data Systems. *Recommendation for Space Data System Standards Space Packet Protocol*. CCSDS Secretariat National Aeronautics and Space Administration, 'Jun' 2020.

- [23] NASA Marshall Space Flight Center. Fly with trek. Web, n.d. Accessed 11 Dec 2023.
- [24] MMA Design LLC. Solar array products. Web, Oct 2023. Accessed 9 Dec 2023.
- [25] Michael Hauge, E. Glenn Lightsey, Mason Starr, Shan Selvamurugan, Graham Jordan, John Cancio, and Conner Awald. Operations systems engineering for the lunar flashlight mission. In *Proceedings of the Small Satellite Conference SSC23-WVII-02*, 2023.